

## Experimental acute anti-inflammatory activity of preparations with complexed cannabidiol in carriers

Daniel Ribeiro Grijó<sup>1\*</sup>, Edvalkia Magna Teobaldo da Rocha<sup>2</sup>,  
Vitor de Cinque Almeida<sup>3</sup>, Ciomar Aparecida Bersani Amado<sup>2</sup>,  
José Eduardo Olivo<sup>1</sup>, Oswaldo Curty da Motta Lima<sup>1</sup>

<sup>1</sup>Departamento de Engenharia Química, Universidade Estadual de Maringá, Maringá, Brasil,

<sup>2</sup>Departamento de Farmacologia e Terapêutica, Universidade Estadual de Maringá, Maringá,

Brasil, <sup>3</sup>Departamento de Química, Universidade Estadual de Maringá, Maringá, Brasil

Cannabidiol (CBD) is a bioactive compound with promising anti-inflammatory results but has low aqueous solubility. Complexation of drugs with this characteristic in carriers is an alternative to improve their efficiency. This study aimed to prepare and characterize CBD complexes in different carriers, and to evaluate the anti-inflammatory effect of such preparations using an experimental model of edema induction in rat paws. The results were compared to a reference drug, ibuprofen (IBU). The carriers evaluated were beta cyclodextrin (bCD) and activated charcoal (AC). Quantification of the drugs in the complexes was determined, and different qualitative analyses were also performed. Oral treatments in single doses with CBD showed inhibitory effects similar to that of IBU, potentiating its bioactivity without significant adverse effects. CBD\*bCD doses at 4.375, 8.75, 17.5, and 35 mg/kg significantly reduced the intensity of edema compared to equivalent doses of pure bioactive. In contrast, CBD\*AC did not generate benefits. There was no significant inhibitory effect on myeloperoxidase activity, requiring more specific analyses to assess this parameter. The results suggest that the CBD\*bCD complexation is perfectly feasible, increasing its anti-edematogenic efficacy in the experimental model used.

**Keywords:** Cannabidiol. Beta cyclodextrin. Activated charcoal. Anti-inflammatory activity.

### INTRODUCTION

Cannabidiol (CBD) is a specific substance obtained from plants of the *Cannabis* genus that are called cannabinoids. Its distinct medicinal application and absence of significant adverse effects were recently evaluated in a broad scientific review carried out by the World Health Organization (WHO, 2018), which later contributed to the recognition of the medicinal potential of the plant by the United Nations (UNODC, 2020).

The anti-inflammatory activity of CBD is one of its most outstanding biological properties. Costa *et al.* (2004; 2007) demonstrated that low doses of this cannabinoid were necessary to induce a good anti-inflammatory

effect in Wistar rats. Bioactive compounds with these characteristics have been studied and evaluated as alternatives to traditional synthetic anti-inflammatory drugs, such as ibuprofen (IBU), as they can produce satisfactory results with a lower risk of adverse effects (Wisniewski-Rebecca *et al.*, 2015). CBD (Garrett, Hunt, 1974), IBU (Friuli *et al.*, 2018), and many other drugs have low aqueous solubility, that is, poor bioavailability when administered neat. An alternative to increase the bioavailability of a drug with this characteristic is to complex it with a biocompatible carrier, allowing a more effective and controlled release/dissolution. The controlled release allows the active concentration of this drug to be maintained within its appropriate therapeutic range for a longer period, promoting a more effective treatment. In addition, it may reduce some adverse effects, since less of the drug is required during treatment (Almeida *et al.*, 2018).

\*Correspondence: D. R. Grijó. Departamento de Engenharia Química (D90). Universidade Estadual de Maringá (UEM). Avenida Colombo 5790, Maringá, Brasil, 87020900. Phone: + 55 44 991 832 007. Email: dr.grijo@gmail.com. ORCID: <https://orcid.org/0000-0002-9312-5974>

Pharmaceutical carriers commonly used are made up of natural or synthetic polymers (Assadpour *et al.*, 2023). Biopolymers called cyclodextrins, formed by  $\alpha$ -1,4-glycosidic bonds between D-glucose monomers, have provided significant increases in the aqueous solubility of cannabinoids. Among these, beta-cyclodextrin (bCD, n=7 monomers) has been the most studied (Mannila *et al.*, 2007; Lv *et al.*, 2019). According to Wittkowski (2017), the purification process for bCD is cheaper and faster than for alpha (n=6) or gamma (n=8) cyclodextrin. Interesting results using activated charcoal (AC) to alternatively carry IBU were obtained in bench studies simulating human conditions (*in vitro*) (Miriyala *et al.*, 2017; Yaneva, 2019). AC has a high ability to interact with drugs due to its large surface area, and, because of its biocompatibility, it is already used in medicine for the treatment of intoxication. In recent years, its production has been based on the use of renewable, safe, cheap, and available in large quantities precursors such as agro-industrial waste (Juurlink, 2016).

*Cannabis*, in addition to being a plant rich in bioactive substances, can be cultivated to obtain high-quality fibers, in which case it is commonly called hemp. Fibers do not have significant levels of cannabinoids and are intended for various industrial applications, such as the production of textiles and composites. The mechanical processing of these fibers generates a low value-added waste called tow (Chandra, Lata, ElSohly, 2017). Studies show that AC produced from hemp fiber derivatives may present larger surface areas and lower production costs compared to other lignocellulosic materials (Dizbay-Onat *et al.*, 2018; Hossain *et al.*, 2018). In addition, other studies have shown that fungi grow exclusively on hemp fibers (Siwulski *et al.*, 2010), which is a promising alternative method to increase the surface area of AC (Wang *et al.*, 2011; Wang *et al.*, 2019).

The present study aimed to prepare and characterize cannabidiol complexes in different carriers (commercial bCD and AC produced from hemp tow) and to evaluate the anti-inflammatory effect of such preparations using the acute inflammation model from the induction of edema in paws of Wistar rats.

## MATERIAL AND METHODS

### Inputs and authorizations

The cannabidiol (CBD) used in this work, manufactured by Isodiol (Iso International, LLC – California/USA), is internationally registered as ISO99™ – Bioactive Anhydrous Hemp Oil™. The product (lot F191106), with a purity greater than 99%, was obtained from *Cannabis* plants that have a delta<sup>9</sup>-tetrahydrocannabinol ( $\Delta^9$ -THC) content < 0.3%, regulated by the United States Agricultural Improvement of Act 2018 (USA, 2018). Product packaging details are shown in Figure S1 of the supplemental material. The use of this bioactive in a Doctoral Thesis of the Department of Chemical Engineering of the State University of Maringá, state of Paraná, Brazil, the country where the research was conducted, was authorized by the National Health Surveillance Agency (ANVISA/Brazil), under the internal records AEP 005/2020, AI-468-2020 and AEP 004/2021.

Ibuprofen (IBU), a reference synthetic anti-inflammatory, was purchased from a compounding pharmacy (Pharmakon, CNPJ: 03.446.178/0001-59), and its high purity was confirmed with a Sigma Aldrich primary standard (Product I4883). The beta-cyclodextrin (bCD) used was purchased from Sigma Aldrich (Product C4767) and the activated charcoal (AC) was produced from hemp fiber tow purchased in Brazil (Casa Monteiro, CNPJ: 17.866.832/0001-98). Interestingly, according to the commercial registration number (NCM: 5302.10.90), this fiber tow was not raw material derived from *Cannabis* (NCM: 5302.10.90) (Brazil, 2008) but from some of the plants that are known as “false hemp” (ASTM, 2003).

### Production and characterization of activated charcoal

The proximate composition of the precursor (tow) was gravimetrically analyzed following the D1762-84 Standard (ASTM, 2007). Cadmium (Cd), copper (Cu), iron (Fe), nickel (Ni), and zinc (Zn) heavy metal contents were evaluated by atomic absorption spectroscopy, using previously dried samples (105 °C for 3 h; 1.5 g)

subjected to heating (450 °C for 10 h) and dilution (10 mL concentrated nitric acid and later in distilled water, up to a total volume of 50 mL) (Linger *et al.*, 2002). The tow was also subjected to analysis by Fourier Transform Infrared Spectroscopy and Attenuated Total Reflectance Module (FTIR-ATR), conducted (Bruker, Tensor II) with a resolution of 4 cm<sup>-1</sup> and 128 scans/min in the range between 4,000 and 800 cm<sup>-1</sup>.

The cultivation of *Pleurotus ostreatus* fungi on precursor (hemp tow), before pyrolysis, was evaluated in an attempt to obtain an AC with a larger surface area, as described by Wang *et al.* (2019) with other lignocellulosic matrices. The use of AC as a carrier, as proposed by Miriyala *et al.* (2017) and Yaneva (2019), may be more efficient with these characteristics, due to its greater adsorption capacity. Thus, a smaller amount of its complex will be necessary to obtain the required dose (desorbed drug). The cultivation procedure was carried out using a substrate with 75% moisture stored in an Erlenmeyer flask, obtained from a mixture of 10 g tow (cut with approximately 3 cm) and 30 g distilled water. The amount of 1 g spawns (inoculum seed) was added to the previously sterilized medium (120 °C for 20 min) and the cultivation was conducted in the absence of light at 27 ± 2 °C (Inácio *et al.*, 2015).

AC was produced from the initial carbonization of the sample (15 g) in an inert atmosphere of nitrogen (N<sub>2</sub> at 100 mL/min), at 20 °C/min up to 500 °C and after 1.5 h 20 °C/min up to 850 °C. Subsequently, the inert gas flow was changed to carbon dioxide (CO<sub>2</sub>, 100 mL/min for 1.5 h). Finally, the system was cooled in an inert atmosphere at -40 °C/min. The AC produced was washed with a 0.1 M HCl solution to remove ash and with ultrapure water until pH normalized. Then, it was filtered (cellulose acetate membrane), dried (105 °C for 24 h), and sieved (< 400 mesh). The exact size of the AC was measured using a laser particle analyzer (Bettersizer, S2-WD), and its surface area by nitrogen fission (QuantaChrome, Nova1200).

### Complexation in different carriers

Complexation of CBD (314.47 g/mol) in bCD (1134.98 g/mol) was performed in a molar proportion of

1:2 (Mannila *et al.*, 2007), from the drip of an ethanolic solution of 20 mg CBD/mL in an aqueous solution of 14.5 mg bCD/mL kept under agitation for 6 h. The volumetric ratio of these two solutions was 1:10 (Frömming, Szejtli, 1994). The formed complex was cooled to 5 °C for 1 h, vacuum filtered through a cellulose acetate membrane, and dried at 40 °C for 12 h. The same conditions were used for the complexation of IBU into bCD, however, due to its molecular weight of 206.27 g/mol, the molar ratio was 0.76.

Complexation experiments in AC were initially conducted with the IBU, from a solution of 690 mg/mL (Miriyała *et al.*, 2017). However, the concentration (250 mg/mL) had to be reduced to avoid the formation of crystals on the surface of the complex after vacuum filtration (Figure S2, supplementary material). Complexation of CBD in AC was performed from a solution of 100 mg/mL, due to its lower solubility in ethanol (Cayman, 2015, 2017) and smaller amount available for research. Complexation of each active was carried out by adding 9 mL ethanolic solution containing the active to 500.0 mg of the AC produced, followed by stirring at 200 rpm at 35 °C for 24 h. The complexes formed were vacuum filtered through cellulose acetate membranes and dried at 40 °C for 24 h.

Quantification was conducted on an HPLC with ultraviolet detection (Varian, 920-LC), using a C18 column with 50 x 2.0 mm; 2.8 mm (Varian Pursuit XRs ULTRA) maintained at 30 °C. The mobile phase with a flow rate of 0.5 mL/min was binary A/B, being A water with 0.1% formic acid and B methanol. The gradient of B was 20% for 0.5 min; 20 to 98% between 0.5 and 3.5 min; 98% between 3.5 and 5.5 min; returning to 20% between 5.5 and 7 min; and maintained at 20% up to 13 min. IBU was used as an internal standard in the quantification of CBD and vice versa, from 2 µL injections detected at 220 nm. The different points of each calibration curve were obtained from the mixture of the active solution (between 0.1 and 1.5 mg/mL) and the internal standard (1 mg/mL), in equal volumes (500 µL each).

The complexation efficiency in AC was measured in triplicate from a 10 mg aliquot of the complex added to a 1 mL volumetric flask. The flask volume was completed with ethanol and after 40 min agitation, alternating

between vortexing for 10 s and ultrasonic bath for 5 min, the solution was transferred to a disposable syringe (3 mL) and filtered (hydrophilic PTFE 0.22  $\mu\text{m}$ ). Shoyama *et al.* (1983) demonstrated that a 1:1 methanol/water mixture could be used to analyze the complexation efficiency in bCD since the drug has a high solubility in alcohol and bCD in water. However, suspended solids were observed after mixing a 500 mL sample with a 500 mL internal standard ethanolic solution. Dimethylsulfoxide (DMSO) was chosen to measure the complexation efficiency of drugs in bCD, since it has high compatibility with CBD (Cayman, 2015), IBU (Cayman, 2017), water, and ethanol (Gaylord, 2014).

Complexation was also qualitatively evaluated by FTIR-ATR, X-Ray Diffractometry (XRD), Thermogravimetry (TG), Differential Thermogravimetry (DTG), Differential Scanning Calorimetry (DSC), and using a fusiometer. XRD analyses (Shimadzu LabX 6000) were conducted using  $\text{CuK}\alpha$  radiation and measurements were determined with a voltage of 40 kV, current of 30 mA, rate of  $2^\circ \text{min}^{-1}$ , acquisition time of 1 s, and continuous mode interval of  $5 \leq 2\theta \leq 40$ . The TG, DTG, and DSC analyses were performed on a simultaneous thermal analyzer (STA 449 F3 Jupiter®, NETZSCH) with 5 - 8 mg of each sample in alumina crucibles and a heating ramp from 25 to 900  $^\circ\text{C}$  at  $20^\circ \text{C min}^{-1}$  under  $50 \text{ mL min}^{-1} \text{N}_2$  atmosphere. The experiments in a fusiometer (Gehaka, PF1500) were carried out after inserting the solid samples into capillaries previously sealed with fire, which were subjected to heating from 45 to 300  $^\circ\text{C}$  at a rate of  $20^\circ\text{C/min}$ .

### Anti-inflammatory activity

Anti-inflammatory activity was evaluated in male Wistar rats with body weight from 200 to 220 g. Animals were kept in an appropriate environment with a temperature of  $23 \pm 2^\circ\text{C}$ , a light/dark cycle of 12 h, and free access to water and chow. The treatment was dissolved in carboxymethylcellulose (CMC 0.5%) and administered as a single oral dose 1 h before the induction of the inflammatory response. Rats were divided into 22 groups: (i) untreated; (ii) CMC; (iii; iv; v) 8.75; 17.5; 35 mg IBU  $\text{kg}^{-1}$ ; (vi) AC; (vii; viii) 8.75; 17.5 mg IBU

complexed in AC  $\text{kg}^{-1}$ ; (ix) bCD; (x; xi; xii) 8.75; 17.5; 35 mg IBU complexed in bCD  $\text{kg}^{-1}$ ; (xiii; xiv; xv) 8.75; 17.5; 35 mg CBD  $\text{kg}^{-1}$ ; (xvi; xvii; xviii) 8.75; 17.5; 35 mg CBD complexed in AC  $\text{kg}^{-1}$ ; (xix; xx; xxi; xii) 4.375; 8.75; 17.5; 35 mg CBD complexed in bCD  $\text{kg}^{-1}$ . Pure doses were defined considering similar studies in the literature (Costa *et al.*, 2004; Wisniewski-Rebecca *et al.*, 2015). The animal care, research, and euthanasia protocols followed the principles and guidelines adopted by the Brazilian College of Animal Experimentation (COBEA). All experimental procedures were approved by the Animal Research Ethics Committee of the State University of Maringá (CEUA/UEM 7125020919 and CEUA/UEM 4591170220).

The animals received an intraplantar injection (intradermal) of 100  $\mu\text{L}$  carrageenan solution (200  $\mu\text{g/paw}$ ) in the left hind paw to induce the inflammatory response. The same volume of vehicle (100  $\mu\text{L}$  0.9% saline solution) was injected into the right hind paw. The volume of both paws was determined using a digital plethysmograph (Ugo Basile<sup>®</sup>), before the induction of the response and 1, 2, and 4 hours after the application of the injurious stimulus. The edema volume was calculated by the difference between the increase in volume of the left hind paw and the increase in volume of the right hind paw:

$$V_t = (V_{L_t} - V_{L_0}) - (V_{R_t} - V_{R_0})$$

where:  $V_{L_t}$  is the volume of the left hind paw after a certain time;  
 $V_{L_0}$  is the volume of the left hind paw prior to the induction;  
 $V_{R_t}$  is the volume of the right hind paw after a certain time;  
 $V_{R_0}$  is the volume of the right hind paw prior to the induction.

The effective dose that reduces the inflammatory response by 50% compared to the control value (mean effective dose,  $\text{ED}_{50}$ ) was estimated for each treatment by non-linear regression (Abotsi *et al.*, 2017), based on the result expressed 4 h after edema induction.

Myeloperoxidase (MPO) activity was evaluated using the homogenate supernatant of the plantar tissue.

At the end of the experimental period (4 h), animals were anesthetized and euthanized using a high dose of isoflurane (5%). The left paw tissue was collected and placed in an Eppendorf tube containing 0.6 mL phosphate-buffered saline solution (PBS, 4 mM, pH 5.4). The sample was homogenized using a Potter homogenizer and centrifuged at 6,000xG, 4 °C for 15 min. The supernatant (0.1 mL) was placed in a 96-well microplate, in triplicate, and then 2.9 mL of a 50 mM PBS solution, pH 6, containing 0.19 mg/mL O-dianidisine dihydrochloride and 0.0005% hydrogen peroxide, was added. The reaction was quenched with a 1.46 M sodium acetate solution (pH 3) and the enzyme activity was determined by the end-point technique, by measuring the absorbance at a wavelength of 460 nm.

Results were presented as mean  $\pm$  standard error of the mean (S.E.M.). Data were tested by analysis of variance (ANOVA), followed by Tukey's test. The significance level was set at  $P < 0.05$ .

## RESULTS AND DISCUSSION

### Production and characterization of activated charcoal

The hemp fiber tow used as a precursor for the production of AC showed  $8.74 \pm 0.06$  % moisture,  $71.77 \pm 0.01$  % other volatiles,  $0.91 \pm 0.05$  % ash, and  $18.57 \pm 0.13$  % fixed carbon. The levels were close to those described in the literature for *Cannabis* fibers, although the raw material used was possibly a "false hemp". Pejic *et al.* (2008) described a moisture content of 8.2%. Branca, Di Blasi, Galgano (2017) described an ash content of 0.6%, despite a lower fixed carbon content (4.9%). Marrot *et al.* (2021) observed significant variations in the proximate composition of raw materials derived from hemp stem. The composition of heavy metals copper, zinc, cadmium, nickel, and iron were, respectively,  $1.71 \pm 0.35$ ,  $34.95 \pm 0.30$ ,  $1.42 \pm 0.09$ ,  $1.32 \pm 0.24$ , and  $178.12 \pm 0.58$  ppm, with correlation coefficients  $R^2 \geq 0.9990$ . The copper composition was close to that described

by Angelova *et al.* (2004) ( $1.7 \cong 1.8$  ppm), but zinc and cadmium were slightly higher ( $35.0 > 18.9$  and  $1.4 > 0.4$ , respectively). The nickel composition was slightly lower than described by Linger *et al.* (2002) ( $1.3 < 6.9$ ) and the iron composition was the highest among the heavy metals analyzed ( $Fe > Zn > Cu > Ni$ ), as described by Khan *et al.* (2008). The sample mass lost during calcination was  $98.57 \pm 0.01$ %.

The FTIR-ATR spectrum of hemp fiber tow is illustrated in Figure S3 (Supplemental Material). As observed here, and corroborating Garside, Wyeth (2003), this technique is not the most suitable for distinguishing natural lignocellulosic fibers such as sisal, ramie, jute, flax, cotton, and hemp. However, the spectral bands observed in the present study, related to functional groups of hemicellulose at 2,918 and 2,850  $cm^{-1}$ , lignin at 1,736 and 1,622  $cm^{-1}$ , and cellulose at 665, 608, 559, and 519  $cm^{-1}$ , are similar to those reported by Yang *et al.* (2007).

Table I lists the adsorbents produced, describing the experimental conditions used and the results obtained. Previous tests on fiber supplementation for the cultivation of *Pleurotus* were conducted, but no significant changes in fungal development were detected (Figure S4, supplemental material). Charcoal production from pure tow (Batch #1) and tow subjected to fungi pre-treatment without supplementation (Batch #2) was evaluated, but there was no significant increase in porosity as reported by Wang *et al.* (2019). The low lignin content of tow, external fibers of hemp stalks (Morin-Crini *et al.*, 2018), is an important factor that differentiated it from the raw material used in this reference study. In addition, Siwulski *et al.*, (2010) tested and evidenced good fungal development only in internal fibers of hemp stalks. Thus, it was decided to produce AC from the precursor without pre-treatment and consequently without autoclaving (Batch #3). Later experiments were carried out from the AC obtained from pyrolysis with optimized parameters using a greater amount of tow (scale-up, Batch #4-5), which resulted in an increase in yield with a smaller surface area.

**TABLE I** – Adsorbents produced from the pyrolysis of different hemp tow samples

CONDITIONS / RESULTS	Batch#1	Batch#2	Batch#3	Batch#4	Batch#5
Sterilization (120°C, 20 min)	yes	yes	no	no	no
Pre-treatment with <i>Pleurotus</i>	no	yes	no	no	no
Initial mass of precursor (g)	15.29	15.30	15.33	25.02	60.09 ± 0.01
Carbonization (N <sub>2</sub> ; 500°C; 2h)	yes	yes	yes	yes	yes
Activation (CO <sub>2</sub> ; 850°C; 1.5h)	no	no	yes	yes	yes
Mass Yield (%)	16.55	22.42	7.12	10.53	14.97 ± 0.46
Adsorbent area, A <sub>BET</sub> (m <sup>2</sup> /g)	101.42	118.44	787.29	474.05	
Micropore area (m <sup>2</sup> /g)	93.13	116.41	646.31	425.37	
External surface area (m <sup>2</sup> /g)	8.29	2.03	140.99	48.68	
Total pore volume (cm <sup>3</sup> /g)	0.063	0.053	0.517	0.309	
Micropore volume (cm <sup>3</sup> /g)	0.052	0.056	0.298	0.231	
Average pore size (nm)	2.50	1.79	2.63	1.31	

Figure 1a shows the nitrogen adsorption and desorption isotherms of the chosen AC (Batch #4-5). There were no large variations in the volume of adsorbed N<sub>2</sub> with the gradual increase in the relative pressure of the system. According to Sing *et al.* (1985), this is a characteristic of a microporous adsorbent. However, a subtle hysteresis during nitrogen desorption was observed, which characterizes the presence of mesopores. These characteristics corroborate the data presented in Table I.

The pore size distribution is shown in Figure 1b. The data (in red) show that 75% of the pores of the AC

produced are micropores, as described in Table I. The predominance of micropores is also evidenced because the largest peaks of the size distribution (in blue) are in the range smaller than < 2 nm. According to Thongpat *et al.* (2021), microporous activated carbons are suitable for adsorbing gaseous and non-drug molecules. Figure 1c shows the result obtained from the laser particle size analyzer. Particles with 38 µm, directly related to the 400-mesh sieve, represent the majority of the AC produced. However, although all particles had previously passed through this sieve, only 45.12% had the expected size, ≤ 38 µm. Actually, the particle size ranged from 2 to 200 µm.

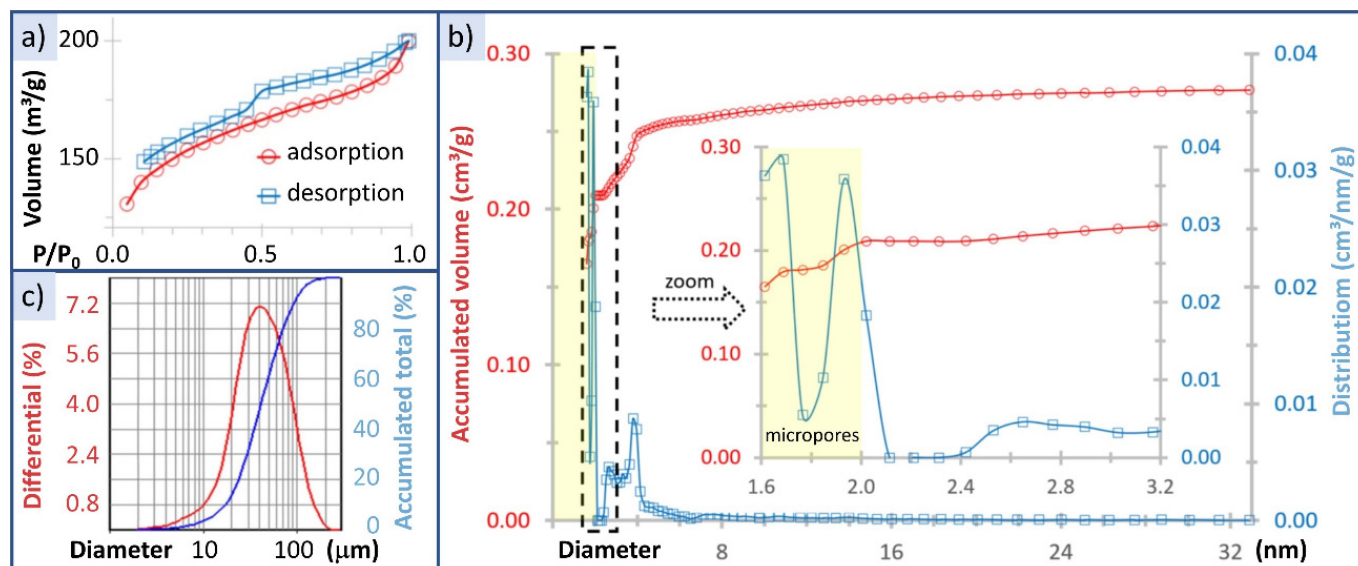


**FIGURE 1** – Characteristics of the AC produced: a) nitrogen adsorption and desorption isotherms, indicating microporous adsorbent with the presence of mesopores (hysteresis); b) pore size distribution, showing the majority presence of micropore (< 2 nm, yellow zone); c) particle size, mostly close to 38  $\mu m$  (400 mesh sieve).

### Complexation in different carriers

The experiments using ethanolic solutions of the 20 mg actives/mL showed the possibility to complex a higher content of CBD in bCD (22.90% w/w) than IBU (11.33% w/w). Quantitative HPLC results were obtained from calibration curves with  $R^2 \geq 0.9937$ . A direct comparison of the complexation content of the two drugs in AC cannot be made because the preparation method was different, but a content (w/w) of 3.96% of CBD and 11.20% of IBU was obtained.

Figures 2-4 qualitatively demonstrate the complexation of CBD in the carriers. Similar results obtained from the IBU are shown in Figures S5-S7 of the supplemental material. In the FTIR-ATR analysis, the spectral bands 3,517; 3,071, and 1,377  $cm^{-1}$  allow the differentiation of CBD from its psychotropic isomer  $\Delta^9$ -THC, based on comparisons with previous studies (SWGDRUG, 2005). According to Lin-Vien *et al.* (1991), these spectral bands refer to the groups -OH, =CH<sub>2</sub>, and C-CH<sub>3</sub>, respectively. Additionally, it was possible to confirm the complexation of the bioactive from the dotted spectral bands present in the complexes and absent in the pure carriers.

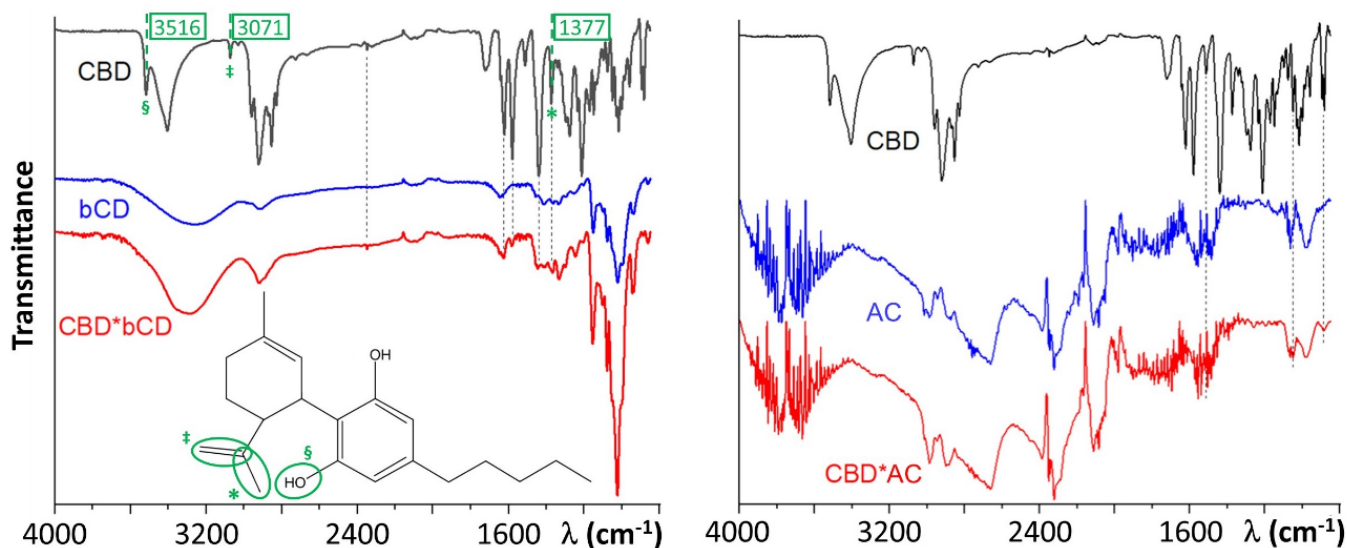


**FIGURE 2** – FTIR-ATR spectra demonstrating CBD complexation in carriers (bCD and AC), also showing in green the spectral bands of the bioactive that allow to differentiate it from its psychotropic isomer D<sup>9</sup>-THC (§ 3517 cm<sup>-1</sup> -OH, ‡ 3071 cm<sup>-1</sup> =CH<sub>2</sub>, and \* 1377 cm<sup>-1</sup> C-CH<sub>3</sub>).

The XRD spectrum obtained from the CBD sample showed crystallinity peaks with the values of 2θ (2θ) 9.82, 10.32, 16.70, 17.48, 19.66, 20.66, 22.22, and 22.78, similar to those described by Vlad *et al.* (2021). Crystallinity of the pure drugs (CBD and IBU) was not observed in both complexes (with AC and with bCD),

confirming the efficiency of complexation procedures. The main crystallinity peaks of IBU (2θ = 6.14, 16.82, 18.82, 19.12, 20.24, 22.44) are different from those of CBD, demonstrating that the technique can distinguish the two pure drugs.

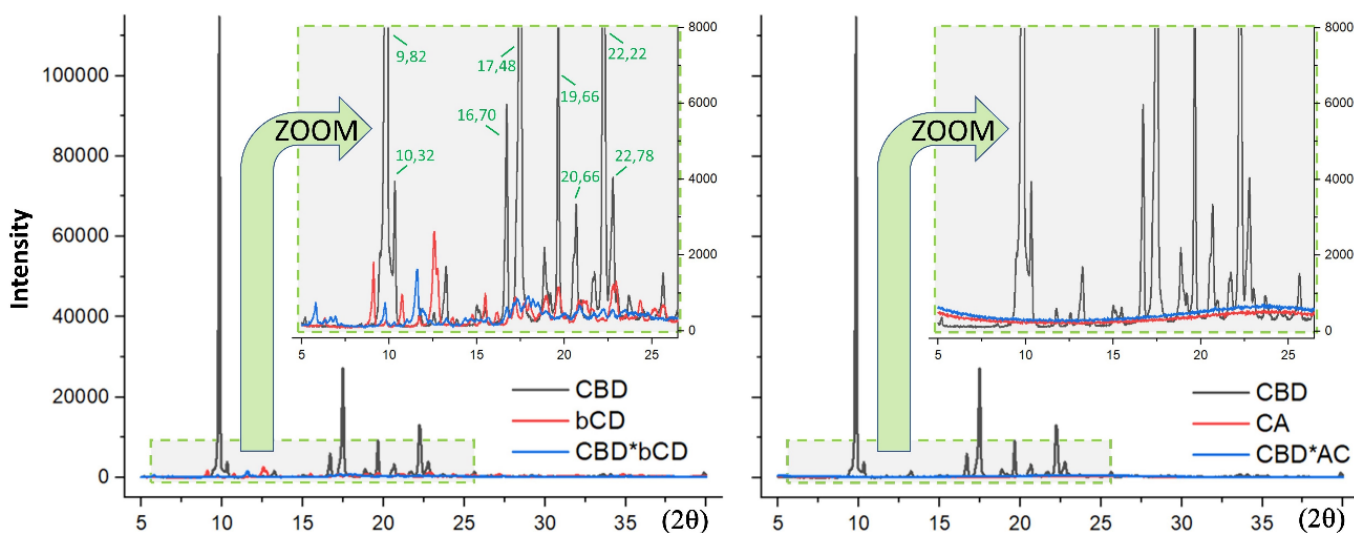


**FIGURE 3** – XRD spectra demonstrating CBD complexation in carriers (bCD and AC).

Thermal analysis via DSC showed that the melting temperature of CBD and IBU is, respectively, 73.11 and 80.33 °C, and the enthalpy of melting of both, -27 and -24 kJ/mol, is endothermic. The results obtained with the fusiometer showed that the melting temperature of CBD is 70.5 °C and of IBU is 79.7 °C, both slightly lower than those obtained via DSC. Furthermore, the TG plot of pure bCD demonstrates a mass loss at temperatures below 100 °C. Abarca *et al.* (2016) demonstrated that this can be

attributed to the evaporation of surface water commonly present in this carrier. The absence of a melting peak of the complexes with bCD proves that there was an improvement in their thermal stability. The characteristics of the degradation range of pure bCD and its complexes are different, proving the complexation of drugs. AC does not show peaks of phase change or abrupt degradation, as expected, and no melting peaks of its complexes are observed, also proving the increase in thermal stability.

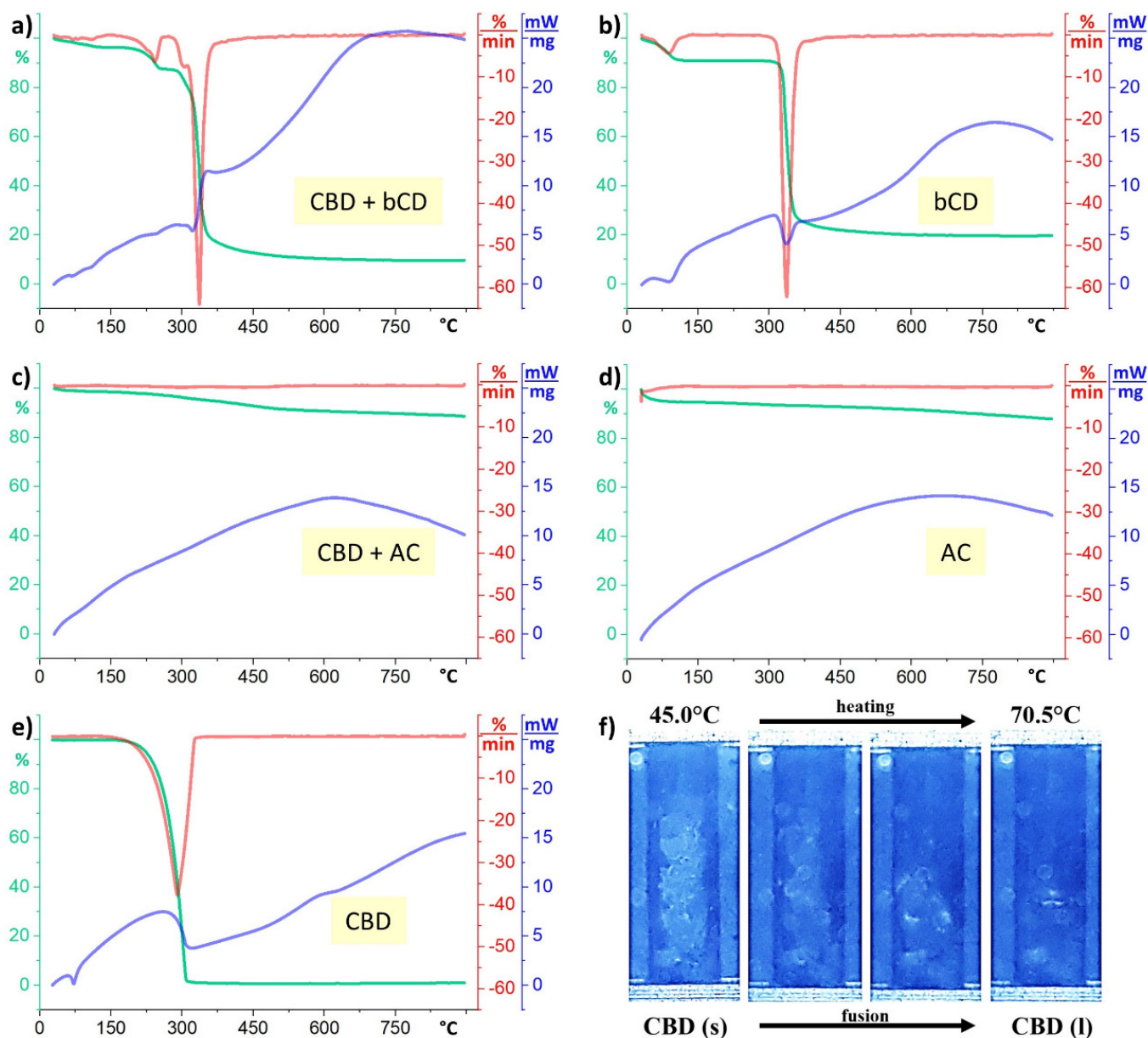


**FIGURE 4** – Thermal analysis of pure and/or complexed CBD: a-e) via Thermogravimetry (TG in %, green), Differential Thermogravimetry (DTG in %/min, red) and Differential Scanning Calorimetry (DSC in mW/mg, blue); f) via fusiometer.

### Effect of treatment with pure or complexed drugs on carrageenan-induced acute inflammatory response

Intraplantar injection of carrageenan provoked a local inflammatory response manifested by edema

formation and an increase in the number of leukocytes recruited at the injury site, mainly neutrophils indirectly determined by the increase in MPO activity, corroborating other studies (Wisniewski-Rebecca *et al.*, 2015; Strzepa, Pritchard, Dittel, 2017; Almeida *et al.*, 2018). These results are presented in Figure 5-7.

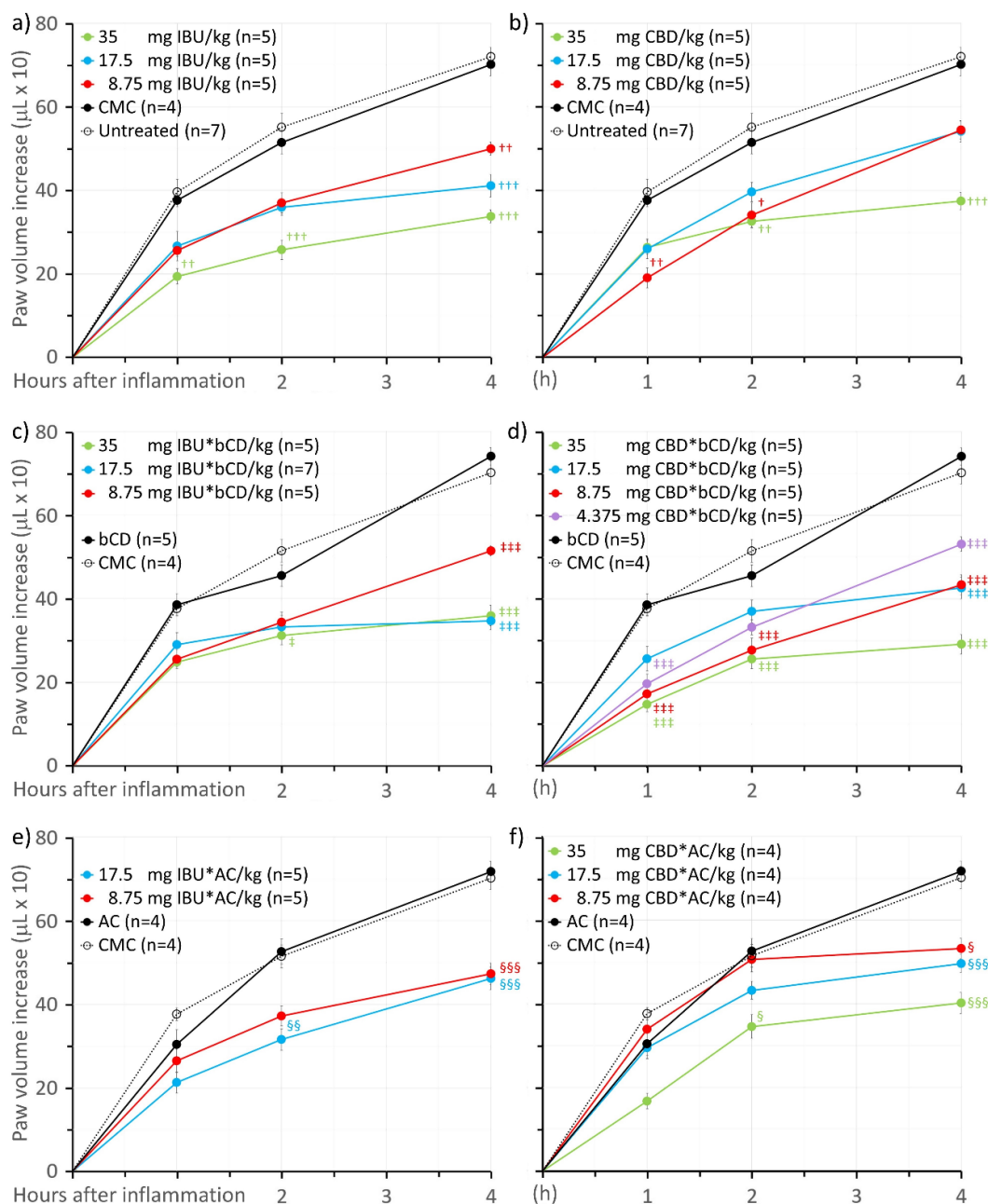


**FIGURE 5** – Effect of treatments on the development of carrageenan-induced paw edema in Wistar rats: a) ibuprofen (IBU); b) cannabidiol (CBD); c) ibuprofen complexed in beta cyclodextrin (IBU\*bCD); d) cannabidiol complexed in beta cyclodextrin (CBD\*bCD); e) ibuprofen complexed in activated charcoal (IBU\*AC); f) cannabidiol complexed in activated charcoal (CBD\*AC). Notes: The treatment was administered orally, in a single dose, 1 h prior to the intraplantar injection of carrageenan (200  $\mu\text{g}$ /paw) in one of the hind paws; The volumes are expressed as the mean  $\pm$  standard error of mean (4 to 7 animals/group). ANOVA by Tukey’s test: †p  $\leq$  0.05, ‡p  $\leq$  0.01, and ###p  $\leq$  0.001, compared with the control group (CMC = †; bCD = ‡; AC = §).

Figure 5a shows a significant inhibitory effect on induced edema obtained with all tested doses (8.75, 17.5, and 35 mg/kg) of pure IBU, corroborating Wisniewski-Rebecca *et al.* (2015). Figure 5b shows that the treatment with pure CBD also inhibited the intensity of edema, being proportional to the utilized dose. Although the CBD at a dose of 8.75 mg/kg significantly reduced the formation of edema 1 h after the carrageenan injection, this effect was not sustained in subsequent hours (2h and 4 h). The highest dose of CBD (35 mg/kg) had a significant inhibitory effect 4 h after the inflammatory response induction. Costa *et al.* (2004) applied daily doses of this bioactive compound using a similar methodology and demonstrated that 40 mg/kg could inhibit 100% edema after four days. These authors demonstrated that lower doses (7.5, 10, and 20 mg/kg) even showed significant inhibitions in the first hours, but after four days they inhibited only about 65% edema. It is important to emphasize that CBD does not have significant adverse effects (WHO, 2018; UNODC, 2020) and that its effective doses for anti-edematogenic action seem to be lower than other promising bioactives, such as anethole (Wisniewski-Rebecca *et al.*, 2015) and curcumin (Almeida *et al.*, 2018).

Figure 5c shows that treatments with the IBU\*bCD complex, at all doses tested (8.75; 17.5, and 35 mg/kg), were similar to the effect of treatments with pure IBU. On the other hand, Figure 5d shows that the treatment of animals with the three doses of CBD complexed in bCD resulted in a greater anti-edematogenic effect compared to the respective doses of pure CBD. Moreover, the effect of treatment with the lowest dose of this complex (4.375 mg

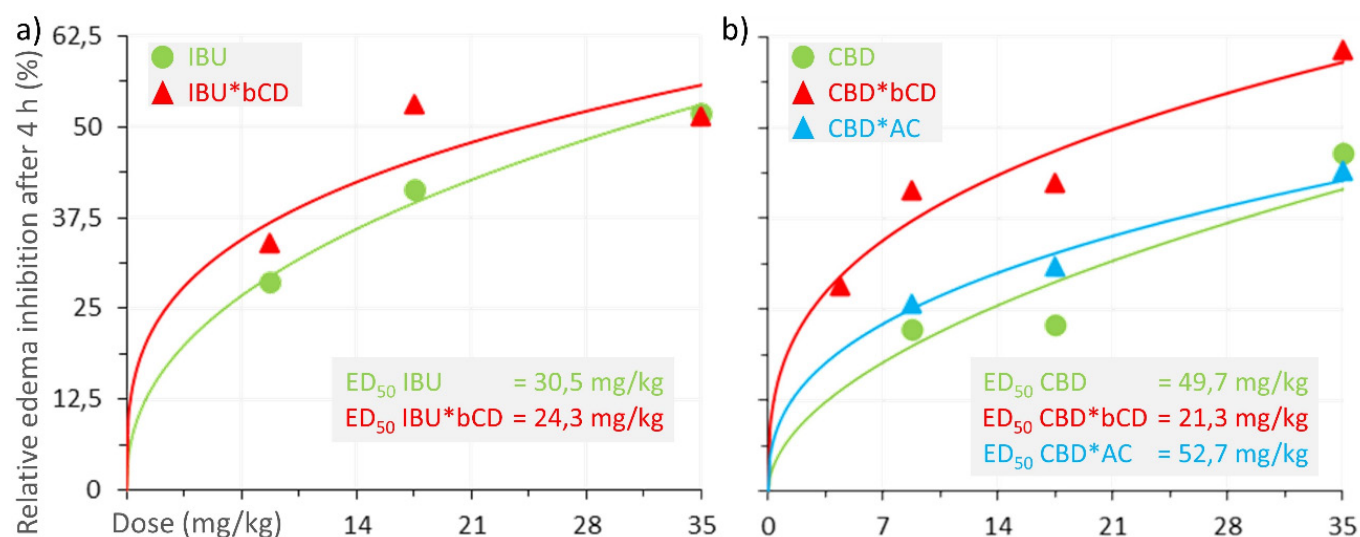
CBD\*bCD/kg) was equivalent to treatment with double the pure bioactive dose (8.75 mg CBD/kg). Figures 5e and 5f show that the inhibitory effects in animals treated with CBD\*AC and IBU\*AC were not significantly different from those treated with pure CBD and IBU.

Table II shows the relative percentages of inhibition of inflammatory edema, obtained after the treatment of rats, of the different groups, with the pure or complexed drugs compared to control groups. Figure 6a shows that the complexation of IBU in bCD caused a small increase in anti-inflammatory activity since the mean effective dose of the pure form was  $ED_{50} \text{ IBU} = 30.5 \text{ mg/kg}$ , and with this complex,  $ED_{50} \text{ IBU*bCD} = 24.3 \text{ mg/kg}$ . Figure 6b shows that the tested doses of pure CBD were not sufficient to generate a 50% inhibition of edema, but that the mean effective dose of this pure bioactive can be estimated at  $ED_{50} \text{ CBD} = 49.7 \text{ mg/kg}$  using the non-linear fit of experimental data. Comparatively, the data demonstrate that pure IBU provided slightly higher anti-inflammatory activity than pure CBD ( $ED_{50} \text{ IBU} < ED_{50} \text{ CBD}$ ). However, there was a more significant increase in anti-inflammatory activity with the complexation of this bioactive in bCD ( $ED_{50} \text{ CBD*bCD} = 21.3 \text{ mg/kg}$ ). CBD complexed in bCD showed higher anti-inflammatory activity than the reference drug complexed in the same carrier ( $ED_{50} \text{ CBD*bCD} < ED_{50} \text{ IBU*bCD}$ ). There was no significant difference in the mean effective dose with the complexation of CBD in AC ( $ED_{50} \text{ CBD} \cong ED_{50} \text{ CBD*AC} = 52.7 \text{ mg/kg}$ ). The  $ED_{50} \text{ IBU*AC}$  was not estimated because only two doses of this treatment were analyzed.

**TABLE II** – Relative percentages of inhibition on the development of paw edema induced by carrageenan in Wistar rats obtained from treatments with pure ibuprofen (IBU) and ibuprofen complexed in beta cyclodextrin (IBU\*bCD) or activated charcoal (IBU\*AC), as well as treatments with pure cannabidiol (CBD) and cannabidiol complexed in beta cyclodextrin (CBD\*bCD) or activated charcoal (CBD\*AC).

Treatment, mg/kg	1 h	2 h	4 h	Treatment, mg/kg	1 h	2 h	4 h
35 IBU †	48%	50%	52%	35 CBD †	30%	37%	47%
17.5 IBU †	29%	30%	41%	17.5 CBD †	31%	23%	23%
8.75 IBU †	32%	28%	29%	8.75 CBD †	49%	34%	22%
35 IBU*bCD ‡	36%	31%	51%	35 CBD*bCD ‡	62%	44%	61%
17.5 IBU*bCD ‡	25%	27%	53%	17.5 CBD*bCD ‡	34%	19%	43%
8.75 IBU*bCD ‡	34%	25%	30%	8.75 CBD*bCD ‡	55%	39%	41%
				4.375 CBD*bCD ‡	49%	27%	28%
				35 CBD*AC §	45%	34%	44%
17.5 IBU*AC §	30%	40%	36%	17.5 CBD*AC §	3%	18%	31%
8.75 IBU*AC §	13%	29%	34%	8.75 CBD*AC §	0%	4%	26%

Note – The treatment was administered orally, in a single dose, 1 h prior to the intraplantar injection of carrageenan (200 µg/paw) in one of the hind paws; Values were calculated in relation to groups of control rats: CMC = † or bCD = ‡ or AC = §.



**FIGURE 6** – Relative percentages of edema inhibition after 4 h of inflammatory induction and their non-linear regressions ( $y=a*(x^b)$ ) to estimate the mean effective dose (ED<sub>50</sub>): a) treatments with pure ibuprofen (IBU R<sup>2</sup>=0.996: a=11.69, b=0.43) and ibuprofen complexed in beta cyclodextrin (IBU\*bCD R<sup>2</sup>=0.952: a=19.25, b=0.30); b) treatments with pure cannabidiol (CBD R<sup>2</sup>=0.939: a=6.33, b=0.53) and cannabidiol complexed in beta cyclodextrin (CBD\*bCD R<sup>2</sup>=0.980: a=18.05, b=0.33) or activated charcoal (CBD\*AC R<sup>2</sup>=0.994: a=10.90, b=0.38).

The effect of different treatments on myeloperoxidase activity, an indirect marker of cell recruitment to the lesion site, can be seen in Figure 7. As observed, none of the treatments significantly reduced MPO activity. The lack of a significant effect on cell recruitment, despite the inhibitory effect on edema, can be explained by considering some factors: the drugs used can inhibit or reduce the production/release of different inflammatory mediators, the model and the experimental protocol selected for the study, the

treatment used (dose, route of administration, time of treatment). Therefore, the hypothesis that both pure and complexed drugs have an inhibitory effect on MPO in other experimental models and longer-term treatment cannot be ruled out. Studies by other authors have shown that CBD treatments in rats reduced plasma levels of prostaglandin E2 (PGE2), cyclooxygenase (COX) activity, production of oxygen-derived free radicals, and nitric oxide concentration in the inflamed paw tissue (Costa *et al.*, 2004; 2007).

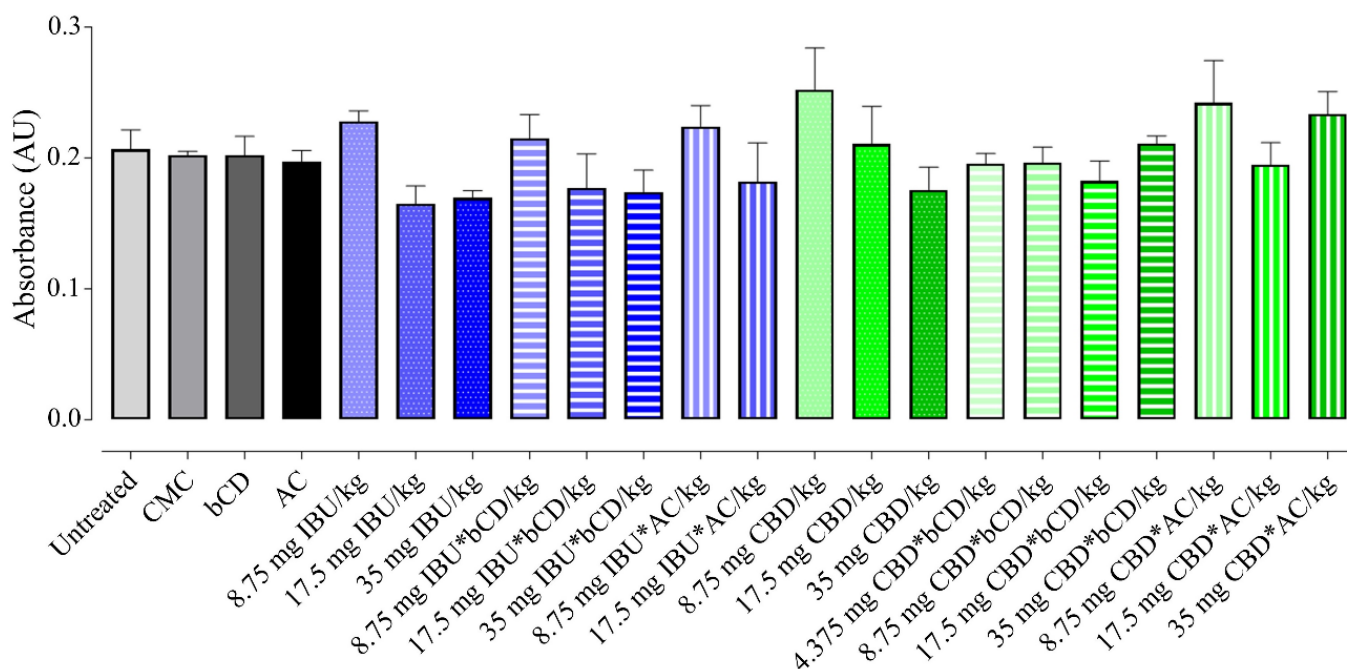


**FIGURE 7** – Effect of treatments with cannabidiol in pure form (CBD), complexed to beta cyclodextrin (CBD\*bCD), and complexed to activated charcoal (CBD\*AC), as well as these respective forms with ibuprofen (IBU, IBU\*bCD, and IBU\*AC), on the myeloperoxidase (MPO) activity in the plantar tissue of Wistar rats. Notes: The treatment was administered orally, in a single dose, 1 h prior to the intraplantar injection of carrageenan (200 µg/paw) in one of the hind paws; The data obtained four hours after edema induction are expressed as the mean ± standard error of the mean (4 to 7 animals/group); There were no statistically variations (ANOVA by Tukey’s test).

## CONCLUSIONS

The hemp fiber derivative used showed physicochemical characteristics similar to those described in the literature, although it may not be a product derived from *Cannabis*. Fungi cultivated on this lignocellulosic material developed significantly without the need for supplementation, but a significant increase in the surface

area of the charcoal was not found under the simplified experimental design analyzed. A more detailed evaluation of these parameters is recommended for a future study, as well as a comparison of results obtained when using external and internal fibers of stalks.

The characterization analyses of the AC produced showed that the adsorbent was predominantly microporous, justifying the low ability to complex

the analyzed drugs. In addition, the complexation methodology requires a large amount of pure active due to its high solubility in solvents such as ethanol. This factor adds an undesirable high cost to the process.

The complexation of the two drugs in bCD was efficient, in which the complexation capacity of CBD in this carrier was greater than that of IBU (22.90 and 11.33% w/w, respectively). This may be related to the lower solubility of CBD in water and ethanol, indicating that this complexation methodology has excellent potential for drugs with low aqueous solubility. XRD was the qualitative technique that best demonstrated results to prove the efficiency of drug complexation in carriers.

In the evaluation of *in vivo* anti-inflammatory activity, pure CBD showed an inhibitory effect on paw edema at similar doses to those of IBU. This important cannabinoid showed a significant increase in inhibitory activity when complexed to bCD, unlike that observed with the reference drug complex. On the other hand, the CBD\*AC complex showed no extra effect compared to the pure bioactive. This demonstrates that bCD is a promising carrier for the development of oral medications with this *Cannabis* derivative.

## ACKNOWLEDGMENTS

We thank the National Council for Scientific and Technological Development (CNPq-Brasil) for granting scholarships and the companies Isodiol and FarmaUSA for providing CBD samples. In addition, the scientific collaboration provided by Jailson Araújo Dantas (UEM/DFT), Laboratory of Adsorption and Ion Exchange (LATI/DEQ/UEM), Multidisciplinary Environmental Study Group (GEMA/UEM), Petroleum and Energy Research Institute from the Federal University of Pernambuco (LITPEG/UFPE) and Laboratory of Planning and Synthesis Applied to Medicinal Chemistry (SINTMED/UFPE).

## REFERENCES

Abarca RL, Rodríguez FJ, Guarda A, Galotto MJ, Bruna JE. Characterization of beta-cyclodextrin inclusion complexes containing an essential oil component. *Food Chem.* 2016;196:968-75.

Abotsi WKM, Lamptey SB, Afrane S, Boakye-Gyasi E, Umoh RU, Woode E. An evaluation of the anti-inflammatory, antipyretic and analgesic effects of hydroethanol leaf extract of *Albizia zygia* in animal models. *Pharm Biol.* 2017;55(1):338–48.

Almeida M, Rocha BA, Francisco CRL, Miranda CG, Santos PDD, de Araujo PHH, et al. Evaluation of the *in vivo* acute antiinflammatory response of curcumin-loaded nanoparticles. *Food Funct.* 2018;9(1):440-9.

Angelova V, Ivanova R, Delibaltova V, Ivanov K. Bio-accumulation and distribution of heavy metals in fibre crops (flax, cotton and hemp). *Ind Crops Prod.* 2004;19(3):197-205.

Assadpour E, Rezaei A, Das SS, Rao BVK, Singh SK, Kharazmi MS, et al. Cannabidiol-Loaded Nanocarriers and Their Therapeutic Applications. *Pharm.* 2023;16(4):487.

ASTM. Standard terminology relating to textiles (d123 - 00b). American Society for Testing and Materials. 2003

ASTM. Standard test method for chemical analysis of wood charcoal. Designation: D1762 – 84 (reapproved). American Society for Testing and Materials. 2007

Branca C, Di Blasi C, Galgano A. Experimental analysis about the exploitation of industrial hemp (*Cannabis sativa*) in pyrolysis. *Fuel Process Technol.* 2017;162:20-9.

Brazil. Sistema Harmonizado de Designação e de Codificação de Mercadorias. Secretaria da Fazenda. Diário Oficial da União 18 jan 2008; Suplemento - Seção 1.

Cayman. Cannabidiol (item nº 90081). Product information [Internet]. 2015 [cited 2023 Jan 19]. Available from: <https://www.caymanchem.com/pdfs/90081.pdf>

Cayman. (±)-ibuprofen (item nº 70280). Product information [Internet]. 2017 [cited 2023 Jan 19]. Available from: <https://www.caymanchem.com/pdfs/70280.pdf>

Chandra S, Lata H, ElSohly MA. *Cannabis sativa* L. - Botany and biotechnology. 1<sup>st</sup> ed. Springer Cham; 2017.

Costa B, Colleoni M, Conti S, Parolaro D, Franke C, Trovato AE, et al. Oral anti-inflammatory activity of cannabidiol, a non-psychoactive constituent of cannabis, in acute carrageenan-induced inflammation in the rat paw. *Naunyn Schmiedebergs Arch Pharmacol.* 2004;369(3):294-9.

Costa B, Trovato AE, Comelli F, Giagnoni G, Colleoni M. The non-psychoactive cannabis constituent cannabidiol is an orally effective therapeutic agent in rat chronic inflammatory and neuropathic pain. *Eur J Pharmacol.* 2007;556:75-83.

Dizbay-Onat M, Vaidya UK, Balanay JAG, Lungu CT. Preparation and characterization of flax, hemp and sisal fiber-derived mesoporous activated carbon adsorbents. *Adsorp Sci Technol.* 2018;36(1-2):441-57.

- Friuli V, Bruni G, Musitelli G, Conte U, Maggi L. Influence of dissolution media and presence of alcohol on the *in vitro* performance of pharmaceutical products containing an insoluble drug. *J Pharm Sci*. 2018;107(1):507-11.
- Frömming KH, Szejtli J. Cyclodextrin inclusion complexes. In: *Cyclodextrins in pharmacy. Topics in Inclusion Science*, vol 5. Springer Dordrecht; 1994:45-82.
- Garrett ER, Hunt CA. Physicochemical properties, solubility, and protein-binding of delta-9-tetrahydrocannabinol. *J Pharm Sci*, 1974;63(7):1056-64.
- Garside P, Wyeth P. Identification of cellulosic fibres by ftir spectroscopy: Thread and single fibre analysis by attenuated total reflectance. *Stud Conserv*. 2003;48(4):269-75.
- Gaylord. Simethyl sulfoxide - solubility data. Bulletin 102 [Internet]. 2014 [cited 2023 Jan 19]. Available from: <https://www.gaylordchemical.com/content/uploads/2020/08/GC-Literature-102B-ENG-Low.pdf>
- Hossain MZ, Wu W, Xu WZ, Chowdhury MBI, Jhavar AK, Machin D, et al. High-surface-area mesoporous activated carbon from hemp bast fiber using hydrothermal processing. *C*. 2018;4(3):38-52.
- Inácio FD, Ferreira RO, Araujo CAV, Peralta RM, Souza CGM. Production of enzymes and biotransformation of orange waste by oyster mushroom, *Pleurotus pulmonarius* (fr.) quél. *Adv Appl Microbiol*. 2015;5(1):1-8.
- Juurlink DN. Activated charcoal for acute overdose: A reappraisal. *Br J Clin Pharmacol*. 2016;81(3):482-7.
- Khan MA, Wajid A, Noor S, Khattak DK, Akhter S, Rahman Iu. Effect of soil contamination on some heavy metals content of *Cannabis sativa*. *J Chem Soc Pak*. 2008;30(6):805-9.
- Linger P, Müssig J, Fischer H, Kobert J. Industrial hemp (*Cannabis sativa* L.) growing on heavy metal contaminated soil: Fibre quality and phytoremediation potential. *Ind Crops Prod*. 2002;16(1):33-42.
- Lin-Vien D, Colthup NB, Fateley WG, Grasselli JG. The handbook of infrared and raman characteristic frequencies of organic molecules. 1<sup>st</sup> ed. Academic Press; 1991.
- Lv P, Zhang D, Guo M, Liu J, Chen X, Guo R, et al. Structural analysis and cytotoxicity of host-guest inclusion complexes of cannabidiol with three native cyclodextrins. *J Drug Deliv Sci Technol*. 2019;51:337-44.
- Mannila J, Järvinen T, Järvinen K, Jarho P. Precipitation complexation method produces cannabidiol/ $\beta$ -cyclodextrin inclusion complex suitable for sublingual administration of cannabidiol. *J Pharm Sci*. 2007;96(2):312-9.
- Marrot L, Candelier K, Valette J, Lanvin C, Horvat B, Legan L, et al. Valorization of hemp stalk waste through thermochemical conversion for energy and electrical applications. *Waste Biomass Valorization*. 2021;13:2267-85.
- Miriyala N, Ouyang DF, Perrie Y, Lowry D, Kirby DJ. Activated carbon as a carrier for amorphous drug delivery: Effect of drug characteristics and carrier wettability. *European Eur J Pharm Biopharm*. 2017;115:197-205.
- Morin-Crini N, Loiacono S, Placet V, Torri G, Bradu C, Kostić M, et al. Hemp-based materials for metal removal. In: *Green adsorbents for pollutant removal: Innovative materials*. Springer International Publishing; 2018:1-34.
- Pejic BM, Kostic MM, Skundric PD, Praskalo JZ. The effects of hemicelluloses and lignin removal on water uptake behavior of hemp fibers. *Bioresour Technol*. 2008;99(15):7152-9.
- Shoyama Y, Morimoto S, Nishioka I. Cannabis. XV. Preparation and stability of  $\delta$ 9-tetrahydrocannabinol- $\beta$ -cyclodextrin inclusion complex. *J Nat Prod*, 1983;46(5):633-7.
- Sing KSW, Everett DH, Haul RAW, Moscou L, Pierotti RA, Rouquerol J, et al. Reporting physisorption data for gas solid systems with special reference to the determination of surface-area and porosity (recommendations 1984). *Pure Appl Chem*. 1985;57(4):603-19.
- Siwulski M, Drzewiecka K, Sobieralski K, Chong Y. Comparison of growth and enzymatic activity of mycelium and yielding of *pleurotus ostreatus* (fr.) kumm. On different substrates. *Acta Sci Pol-Hortoru*. 2010;9(3):45-50.
- Strzepa A, Pritchard KA, Dittel BN. Myeloperoxidase: A new player in autoimmunity. *Cell Immunol*. 2017;317:1-8.
- SWGDRUG. Monographs: Marijuana. Scientific working group for the analysis of seized drugs [Internet]. 2005 [cited 2023 Jan 19]. Available from: <http://www.swgdrug.org/monographs/marijuana.pdf>
- Thongpat W, Taweekun J, Maliwan K. Synthesis and characterization of microporous activated carbon from rubberwood by chemical activation with KOH. *Carbon Lett*. 2021;31(5):1079-88.
- UNODC. Commission on Narcotic Drugs, 63<sup>rd</sup> session: Decision 63/14 (cannabis and cannabis-related substances). United Nations Office on Drugs and Crime [Internet]. 2020 [cited 2023 May 1]. Available from: [https://www.unodc.org/documents/commissions/CND/Drug\\_Resolutions/2020-2029/2020/Decision\\_63\\_14.pdf](https://www.unodc.org/documents/commissions/CND/Drug_Resolutions/2020-2029/2020/Decision_63_14.pdf)
- USA. Public law 115-334. Agriculture improvement Act of 2018. United States of America [Internet]. 2018 [cited 2023 Jan 19]. Available from: <https://www.congress.gov/115/plaws/publ334/PLAW-115publ334.pdf>
- Vlad R-A, Sovány T, Kristó K, Ibrahim YH-EY, Ciurba A, Aigner Z, et al. Structural and thermal analysis of cannabidiol orodispersible formulations. *Farmacia*, 2021;69(3):426-33.

Wang P, Ye H, Yin YX, Chen H, Bian YB, Wang ZR, et al. Fungi-enabled synthesis of ultrahigh-surface-area porous carbon. *Adv Mater.* 2019;31(4).

Wang XM, Xu LJ, Xu JH, Zhang GZ, Wu SB Preparation and capability of activated carbons with high specific surface area by microbial enzymatic and chemical activation. *Trans Tech Publications.* 2011;236-8:225-8.

WHO. Fortieth meeting of the expert committee on drug dependence, 40th ECDD. World Health Organization [Internet]. 2018 [cited 2023 May 1]. Available from: <https://apps.who.int/iris/bitstream/handle/10665/279948/9789241210225-eng.pdf>

Wisniewski-Rebecca ES, Rocha BA, Wiirzler LAM, Cuman RKN, Velazquez-Martinez CA, Bersani-Amado CA. Synergistic effects of anethole and ibuprofen in acute inflammatory response. *Chem Biol Interact.* 2015;242:247-53.

Wittkowski KM. Use of cyclodextrins to reduce endocytosis in malignant and neurodegenerative disorders. Patent No. WO2017163128A2. 2017.

Yaneva ZL. Nonsteroidal anti-inflammatory drug solid-state microencapsulation on green activated carbon - mass transfer and host-guest interactions. *Chem Biochem Eng Q.* 2019;33(2):249-69.

Yang H, Yan R, Chen H, Lee DH, Zheng C. Characteristics of hemicellulose, cellulose and lignin pyrolysis. *Fuel.* 2007;86(12):1781-8.

Received for publication on 21<sup>st</sup> January 2023

Accepted for publication on 19<sup>th</sup> June 2023

## SUPPLEMENTARY MATERIAL



FIGURE S1 – Isodiol CBD packaging details (ISO99TM, 1 g).

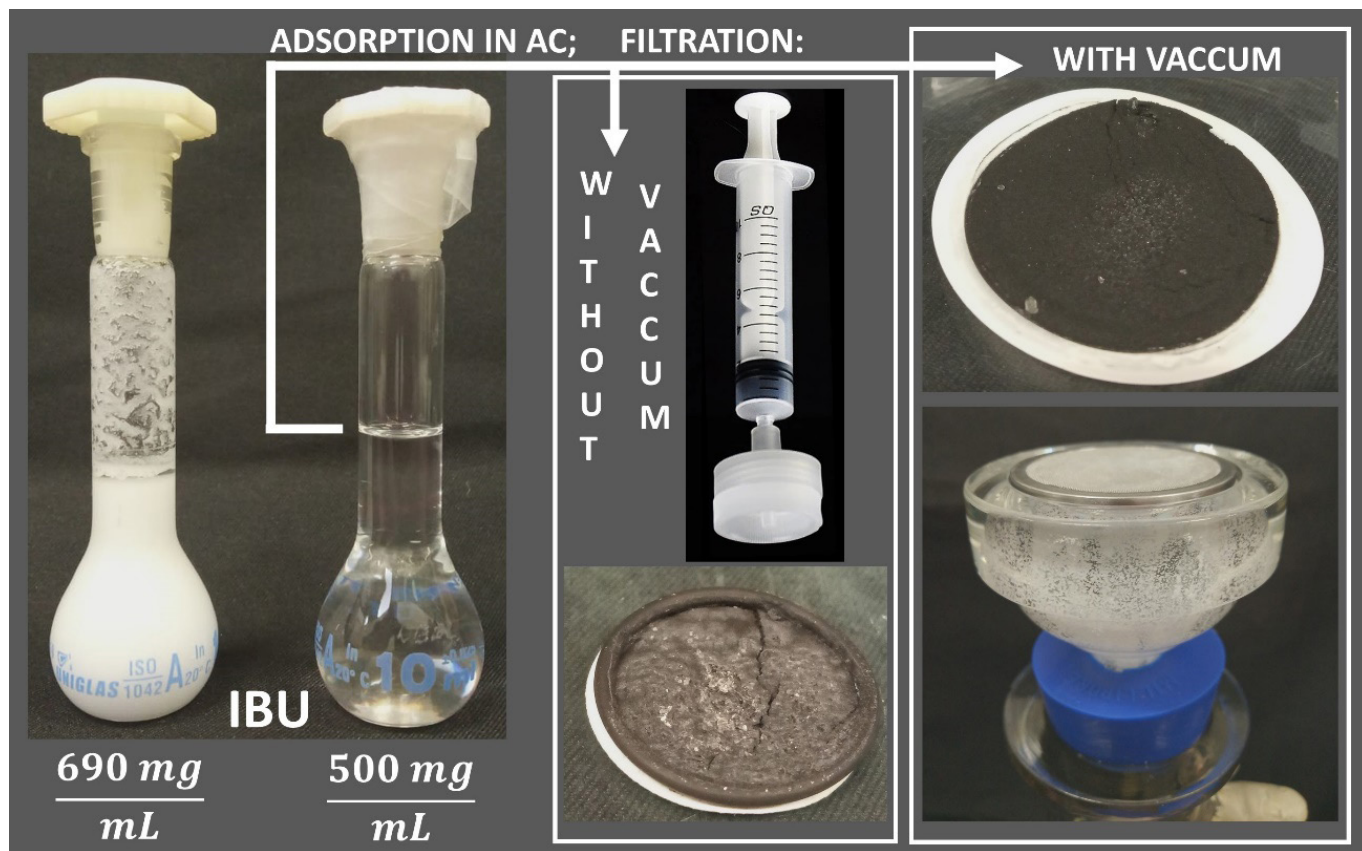


FIGURE S2 – Initial tests of complexation from IBU to AC, evidencing the problematic formation of crystals.

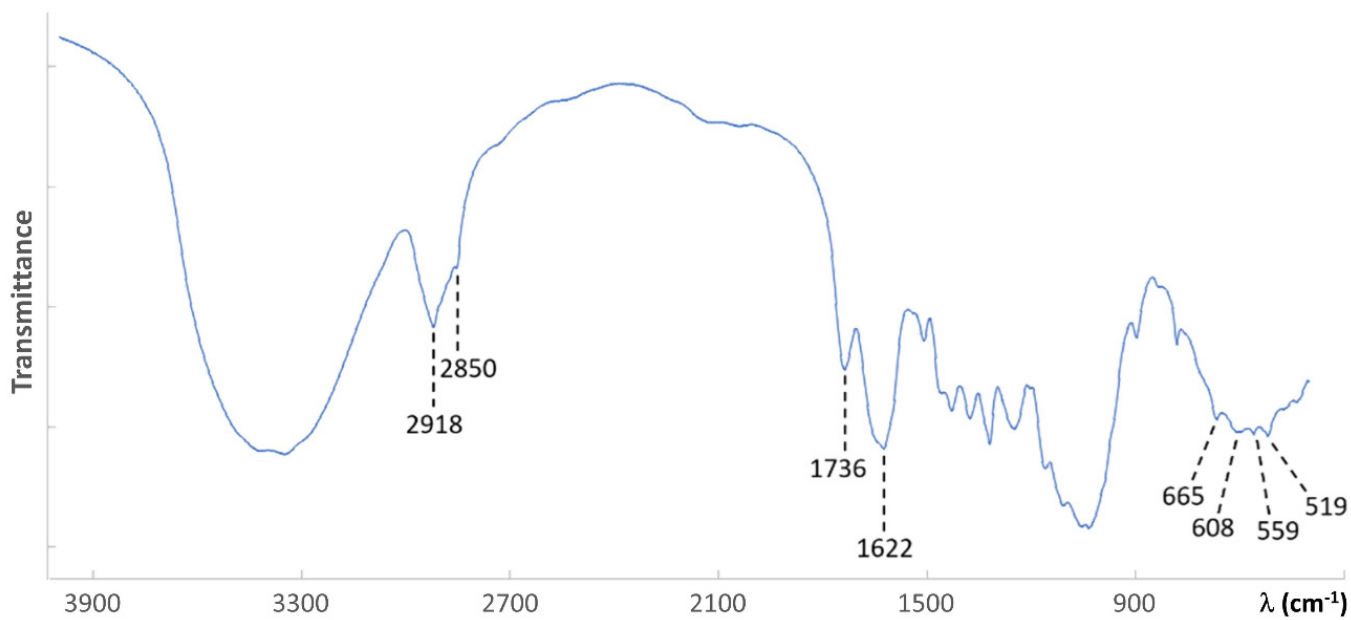
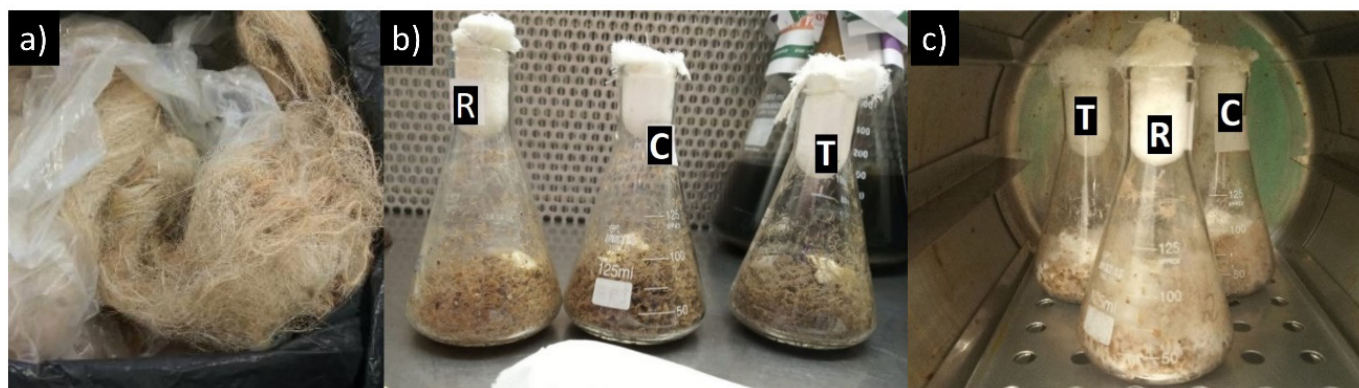
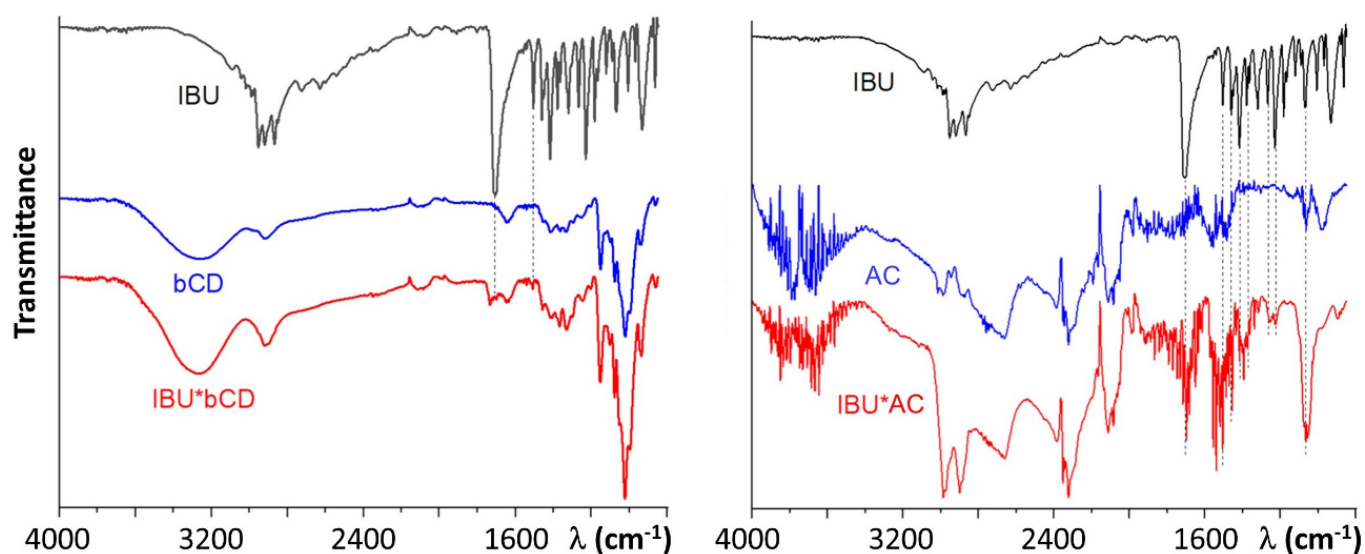


FIGURE S3 – FTIR-ATR spectrum of hemp fiber tow.



**FIGURE S4** – Analysis of the influence of supplementation on the cultivation of *Pleurotus* in hemp tows (T: tow without supplementation; R: tow supplemented with rice bran; C: tow supplemented with Czapek-Dox Broth DIFCO – 30.0 g/L of sucrose, 3.0 g/L of sodium nitrate, 1.0 g/L of dipotassium phosphate, 0.5 g/L of magnesium sulfate, 0.5 g/L of potassium chloride and 0.01 g/L of ferrous sulfate): a) purchased tows; b) after adding approximately 1 g of “spawns”; c) after fungal development for 12 days.



**FIGURE S5** – FTIR-ATR spectra demonstrating IBU complexation in carriers (bCD and AC).

Experimental acute anti-inflammatory activity of preparations with complexed cannabidiol in carriers

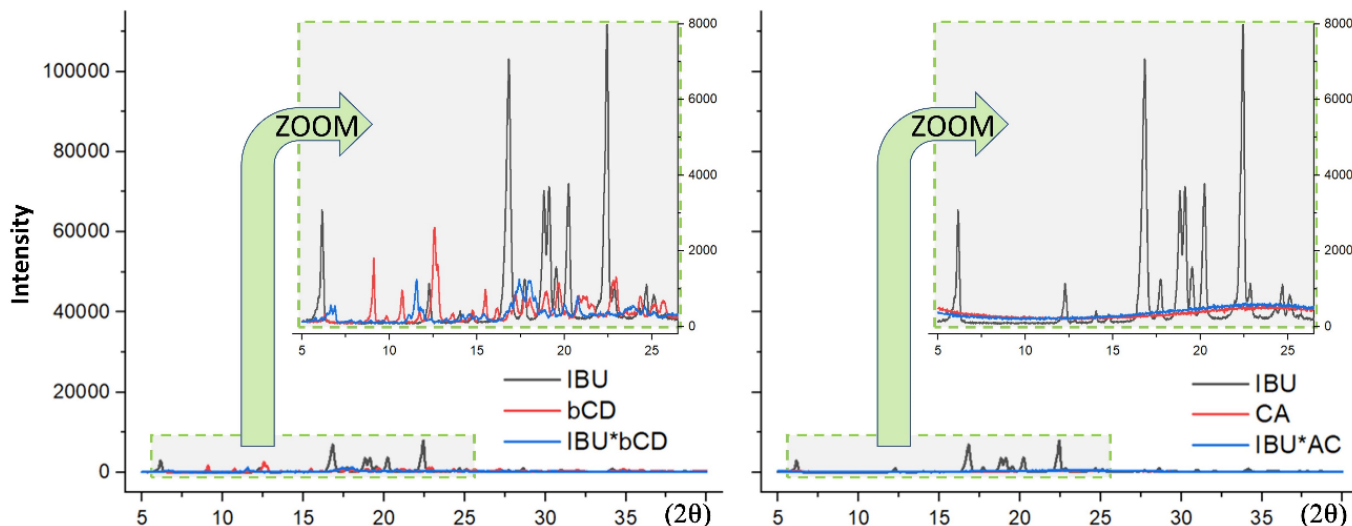


FIGURE S6 - XRD spectra demonstrating IBU complexation in carriers (bCD and AC).

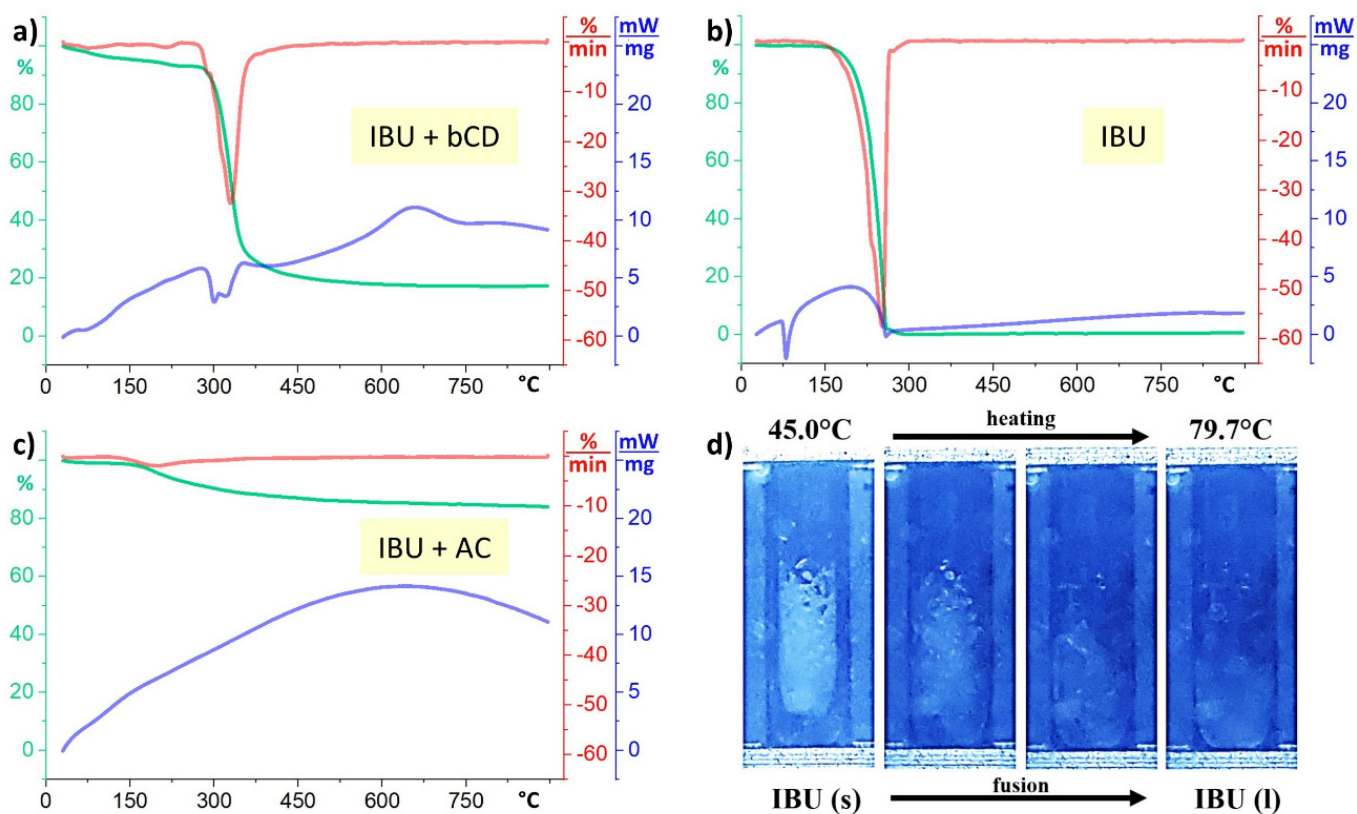


FIGURE S7 – Thermal analysis of pure and/or complexed IBU: a-c) via Thermogravimetry (TG in %, green), Differential Thermogravimetry (DTG in %/min, red) and Differential Scanning Calorimetry (DSC in mW/mg, blue); f) via fusiometer.